Pair correlations of scattered atoms from two colliding Bose-Einstein condensates: Perturbative approach

J. Chwedeńczuk,[1] P. Ziń,[2] M. Trippenbach,[1,2] A. Perrin,[3,4] V. Leung,[3] D. Boiron,[3] and C. I. Westbrook[3]
[1]*Institute of Theoretical Physics, Physics Department, Warsaw University, Hoża 69, PL-00-681 Warsaw, Poland*
[2]*The Andrzej Sołtan Institute for Nuclear Studies, Warsaw University, Hoża 69, PL-00-681 Warsaw, Poland*
[3]*Laboratoire Charles Fabry de l'Institut d'Optique, CNRS, Univ Paris-Sud, Campus Polytechnique, RD128, 91127 Palaiseau cedex, France*
[4]*Atominstitut der Österreichischen Universitäten, TU-Wien, Stadionallee 2, A-1020 Vienna, Austria*
(Received 22 July 2008; published 4 November 2008)

We apply an analytical model for anisotropic, colliding Bose-Einstein condensates in a spontaneous four-wave-mixing geometry to evaluate the second-order correlation function of the field of scattered atoms. Our approach uses quantized scattering modes and the equivalent of a classical, undepleted pump approximation. Results to lowest order in perturbation theory are compared with a recent experiment and with other theoretical approaches.

DOI: 10.1103/PhysRevA.78.053605 PACS number(s): 03.75.Nt, 34.50.Cx

I. INTRODUCTION

The analog of correlated photon pair production [1] has recently been demonstrated using atoms. Both molecular dissociation [2] and four-wave mixing of de Broglie waves [3] have shown correlation peaks. As in quantum optics, such atom pairs lend themselves to investigations into nonclassical correlation phenomena such as entanglement of massive particles [4–7] and spontaneous directionality or superradiant effects [5,8]. From the point of view of the outgoing atoms, the underlying physics is very similar and thus theoretical descriptions should be applicable to both processes. The experiment using four-wave mixing of metastable helium atoms in particular has yielded detailed information about the atomic pair correlations. Efforts to treat the experimental situations are therefore highly desirable.

Theoretically, a description of condensate collisions in the spontaneous scattering regime requires a formulation that extends beyond the mean-field model [9,10]. In previous work on spherical Gaussian wave packets, within a perturbative approach, we have given analytical formulas for the correlation functions [11,12].

In this paper we extend our method to anisotropic condensates to give an analytic description of the correlation properties of spontaneously emitted atom pairs in a geometry much closer to and in good agreement with the experiment [3]. Numerical approaches using the truncated Wigner method [13,14] and positive-P method [15–17] have also been used, in particular to give insight into the stimulation regime where bosonic enhancement comes to play.

Here, we use the model of colliding condensates to examine two types of correlations. First, we shall focus on atom pairs originating from the same two-body scattering event. These consequently have nearly opposite momenta. Thus we analyze the opposite-momenta correlations of atom pairs. Second, we examine two-body correlations between atoms scattered with nearly collinear momenta, a manifestation of the Hanbury Brown-Twiss (HBT) effect [11,15,16,18]. In both cases, the demonstration of a two-particle correlation requires a measurement of the conditional probability of detecting a particle at position $\mathbf{r}_1$ given that a particle was detected at $\mathbf{r}_2$. This probability is proportional to the second-order correlation function $G^{(2)}(\mathbf{r}_1,\mathbf{r}_2)$ of the field $\hat{\delta}$ of atoms: i.e.,

$$G^{(2)}(\mathbf{r}_1,\mathbf{r}_2)=\langle\hat{\delta}^{\dagger}(\mathbf{r}_1)\hat{\delta}^{\dagger}(\mathbf{r}_2)\hat{\delta}(\mathbf{r}_2)\hat{\delta}(\mathbf{r}_1)\rangle.$$

We shall pay particular attention to correlations in momentum space and compare these results with experimental data of [3]. A careful comparison of a numerical treatment based on the positive-P method [17] with the experiment [3] indicated reasonable agreement, but one of the limitations of the method, the short collision duration which could be simulated, left some unresolved questions. In particular, energy conservation is a less stringent constraint for short collision times, and thus one can wonder about the role this constraint plays in the experiment. The treatment given here is not subject to this limitation and also agrees fairly well with the experiment for most of the experimentally accessible observables. One observable quantity, however—the averaged width of the collinear correlation function in a direction orthogonal to the symmetry axis—disagrees with the experiment and with Ref. [17]. In our treatment, it is precisely the requirement of energy conservation that is at the origin of the difference. At the end of the paper we shall discuss possible explanations of this discrepancy.

Let us first describe the experiment in which a collision of two Bose-Einstein condensates of metastable helium produces a cloud of scattered atoms. A condensate of approximately 10^4–10^5 He* atoms is created in a cigar-shaped magnetic trap with axial and radial trapping frequencies of $\omega_z=2\pi\times 47$ Hz and $\omega_r=2\pi\times 1150$ Hz, respectively. Three laser beams are used to transfer the atoms into two counterpropagating wave packets by a Raman process, with a transfer efficiency of about 60%. As the wave packets counterpropagate with a relative velocity of $2v_{\mathrm{rec}}=18.4$ cm/s, atoms from the two clouds collide via s-wave scattering, populating a spherical shell in momentum space often referred to as the "halo" [19–21] (see Fig. 1). In the experiment, about 5% of the atoms are scattered. In addition

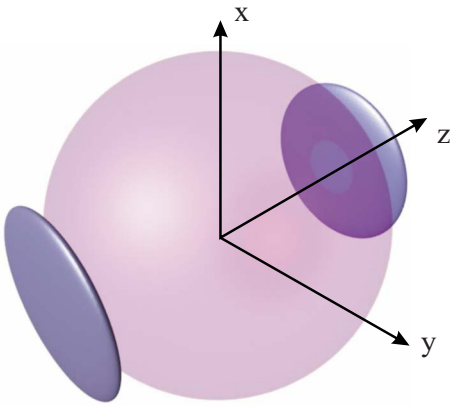

FIG. 1. (Color online) Velocity space representation of the pair production experiment. Raman pulses generate counterpropagating condensates which collide and expand into disk-shaped clouds along the z axis. Atoms scattered during the collision expand to form a spherical shell of correlated pairs. Note that the orientation of the axes in this article differs from Ref. [3]

to splitting the condensate, the Raman transition transfers the atoms into an untrapped magnetic substate. The transferred atoms thus expand freely, falling onto a microchannel plate (MCP) detector that allows the three-dimensional reconstruction of the position of single atoms with an estimated efficiency of 10% [22,23]. Knowing the positions of individual atoms, the initial momenta and the second-order momentum correlation function of the cloud of scattered particles can be computed. The precision of the measurement is limited by the finite resolution of the MCP. This factor will be taken into account in our comparison between the theoretical estimates and the experimental results.

II. MODEL FOR SCATTERING

To make the comparison, we introduce a simplified model for atom scattering during a collision of two Bose-Einstein condensate wave packets. In this model we assume that two counterpropagating wave packets constitute a classical undepleted source for the process of scattering. This concept is introduced in analogy to examples in quantum optics, where a strong coherent laser field is treated as a classical wave and its depletion is neglected [24]. We shall simplify the model further on. Since we assume that the two colliding condensates remain undepleted, the population of the $\hat{\delta}$ field of scattered atoms should be small, as compared to the number of atoms in the condensates. In such a regime, a Bogoliubov approximation is often used [25,26], leading to linearized equations of motion for the quantum fields. In our case, the $\hat{\delta}$ field of scattered atoms satisfies the Heisenberg equation (for details of the derivation, see [11,12])

$$i\hbar\partial_t\hat{\delta}(\mathbf{r},t) = -\frac{\hbar^2\nabla^2}{2m}\hat{\delta}(\mathbf{r},t) + 2g\psi_Q(\mathbf{r},t)\psi_{-Q}(\mathbf{r},t)\hat{\delta}^\dagger(\mathbf{r},t). \tag{1}$$

Here $\psi_{\pm Q}(\mathbf{r},t)$ is the c-number wave function of the colliding condensates with mean momentum per atom equal to $\pm\hbar Q$. Moreover, the coupling constant $g=\frac{4\pi\hbar^2 a}{m}$ is related to the atomic mass m and s-wave scattering length a of He*.

To permit analytic calculations, we model the condensate wave functions $\psi_{\pm Q}(x,y,z,t)$ as Gaussians:

$$\psi_{\pm Q} = \sqrt{\frac{N}{2\pi^{3/2}\sigma_r^2\sigma_z}}\exp\left(\mp iQz - \frac{i\hbar Q^2 t}{2m}\right) \times\exp\left[-\frac{1}{2\sigma_r^2}(x^2+y^2) - \frac{1}{2\sigma_z^2}\left(z \mp \frac{\hbar Q t}{m}\right)^2\right], \tag{2}$$

where N is the total number of particles in both wave packets. The radial (σ_r) and axial (σ_z) width of the Gaussians are extracted from the initial condensate wave function Ψ_0 which is calculated numerically from the Gross-Pitaevski equation using an imaginary-time method. In practice, we fit $\int dv_x\int dv_y|\Psi_0(\mathbf{v})|^2$ with a Gaussian function $\propto\exp(-v_z^2/\chi_z^2)$ and then use $\sigma_z=\hbar/(m\chi_z)$. We define σ_r similarly. Here, for simplicity, we neglect the spread of the condensates during the collision. This assumption seems reasonable because most of the atom collisions take place before the two clouds have had time to expand.

It is useful to change variables and rescale the field operator

$$\frac{\hbar Q}{m\sigma_z}t\to t, \quad \mathbf{r}/\sigma_z\to\mathbf{r}, \quad \frac{1}{\sigma_z^{3/2}}\hat{\delta}(\mathbf{r},t)\to\hat{\delta}(\mathbf{r},t),$$

which simplifies the equation of motion (1): i.e.,

$$i\beta\partial_t\hat{\delta}(\mathbf{r},t) = -\frac{1}{2}\nabla^2\hat{\delta}(\mathbf{r},t) + \alpha e^{-(x^2+y^2)/\gamma^2-z^2}e^{-i\beta t-t^2}\hat{\delta}^\dagger(\mathbf{r},t), \tag{3}$$

where $\alpha=\frac{4Na\sigma_z}{\sigma_r^2\sqrt{\pi}}$, $\beta=Q\sigma_z$, and $\gamma=\frac{\sigma_r}{\sigma_z}$.

The condensate density in momentum space then reads

$$|\Psi_0(\mathbf{k})|^2 = \frac{N\beta^3}{\sqrt{\pi^3}\gamma^2}\exp[-\beta^2(k_z^2+\gamma^2k_r^2)]. \tag{4}$$

The three parameters α, β, and γ fully determine the dynamics of the field of scattered atoms. For $N=10^4$ and $\hbar Q=mv_{\mathrm{rec}}$ we have $\alpha=1652$, $\beta=227$, and $\gamma=0.05$.

We also find $\chi_z=0.004v_{\mathrm{rec}}$, $\sigma_z=39$ μm, $\chi_r=0.0870v_{\mathrm{rec}}$, and $\sigma_r=2$ μm. The parameter α is a measure of the strength of the interactions between particles. As such, it governs the fraction of atoms scattered into the halo. As a consistency check, in Appendix A we give an alternate estimate of α in the experiment using the observed fraction of scattered atoms.

In Sec. III we derive an analytical expression for the second-order correlation function in the perturbative regime. It is still an open question whether, for these parameters, the perturbative approach applies. We tackle this issue after the evaluation of the $G^{(2)}$ function is Sec. III C. In Sec. IV we compare the perturbative results with the experimental data of [3].

III. DERIVATION OF $G^{(2)}$ IN THE PERTURBATIVE REGIME

We shall begin the analytical calculations with a definition of the Fourier transform of the $\hat{\delta}$ operator:

$$\hat{\delta}(\mathbf{r},t)=\left(\frac{\beta}{2\pi}\right)^{3/2}\int d\mathbf{k}e^{i\beta\mathbf{k}\cdot\mathbf{r}-i\beta k^2 t/2}\hat{\delta}(\mathbf{k},t). \tag{5}$$

This particular form of the Fourier transformation "incorporates" the free evolution of the field. Substitution of Eq. (5) into Eq. (3) gives

$$\partial_t\hat{\delta}(\mathbf{k},t)=\mathcal{A}e^{-i\beta t}e^{-t^2}\int d\mathbf{k}'e^{(i\beta/2)(k^2+k'^2)t}\times\exp\left(-\frac{\gamma^2\beta^2}{4}(\mathbf{k}_r+\mathbf{k}_r')^2-\frac{\beta^2}{4}(k_z+k_z')^2\right)\hat{\delta}^\dagger(\mathbf{k}',t),$$

where $\mathcal{A}=-i\frac{\alpha\beta^2\gamma^2}{8\pi^{3/2}}$, $\mathbf{k}_r=k_x\mathbf{e}_x+k_y\mathbf{e}_y$, and $\mathbf{e}_i$ is a unit vector in i direction. The above can be integrated formally, giving

$$\hat{\delta}(\mathbf{k},t)=\mathcal{A}\int_0^t d\tau e^{-i\beta\tau}e^{-\tau^2}\int d\mathbf{k}'e^{(i\beta/2)(k^2+k'^2)\tau}\times\exp\left(-\frac{\gamma^2\beta^2}{4}(\mathbf{k}_r+\mathbf{k}_r')^2-\frac{\beta^2}{4}(k_z+k_z')^2\right)\hat{\delta}^\dagger(\mathbf{k}',\tau).$$

Since in the Heisenberg picture the scattered field remains in its initial vacuum state and the evolution of the $\hat{\delta}$ field is linear, the second-order correlation function $G^{(2)}(\mathbf{k}_1,\mathbf{k}_2)$ decomposes into

$$\begin{aligned}G^{(2)}(\mathbf{k}_1,\mathbf{k}_2;t)&=\langle\hat{\delta}^\dagger(\mathbf{k}_1,t)\hat{\delta}^\dagger(\mathbf{k}_2,t)\hat{\delta}(\mathbf{k}_2,t)\hat{\delta}(\mathbf{k}_1,t)\rangle\\&=G^{(1)}(\mathbf{k}_1,\mathbf{k}_1;t)\cdot G^{(1)}(\mathbf{k}_2,\mathbf{k}_2;t)\\&\quad+|G^{(1)}(\mathbf{k}_1,\mathbf{k}_2;t)|^2+|M(\mathbf{k}_1,\mathbf{k}_2;t)|^2,\end{aligned} \tag{6}$$

where $M(\mathbf{k}_1,\mathbf{k}_2;t)=\langle\hat{\delta}(\mathbf{k}_1,t)\hat{\delta}(\mathbf{k}_2,t)\rangle$ is the anomalous density and $G^{(1)}(\mathbf{k}_1,\mathbf{k}_2;t)=\langle\hat{\delta}^\dagger(\mathbf{k}_1,t)\hat{\delta}(\mathbf{k}_2,t)\rangle$ is the first-order correlation function. Below we calculate these two functions in the lowest order and for a time $t=\infty$ because all the measurements are made long after the collision has finished. We expand $\hat{\delta}$ in a series of perturbative solutions,

$$\hat{\delta}(\mathbf{k},t=\infty)=\sum_{i=0}^{\infty}\hat{\delta}^{(i)}(\mathbf{k}),$$

where to the lowest order we get

$$\hat{\delta}^{(1)}(\mathbf{k})=\mathcal{A}\int_0^\infty d\tau e^{-i\beta\tau}e^{-\tau^2}\int d\mathbf{k}'e^{(i\beta/2)(k^2+k'^2)\tau}\times\exp\left(-\frac{\gamma^2\beta^2}{4}(\mathbf{k}_r+\mathbf{k}_r')^2-\frac{\beta^2}{4}(k_z+k_z')^2\right)\hat{\delta}^{(0)\dagger}(\mathbf{k}'). \tag{7}$$

A. Anomalous density: $\mathbf{k}_1\simeq-\mathbf{k}_2$ correlations

The anomalous density to the first order is expressed as

$$M(\mathbf{k}_1,\mathbf{k}_2)=\langle\hat{\delta}^{(0)}(\mathbf{k}_1)\hat{\delta}^{(1)}(\mathbf{k}_2)\rangle.$$

Using Eq. (7) we get

$$\begin{aligned}M(\mathbf{k}_1,\mathbf{k}_2)&=\mathcal{A}\exp\left(-\frac{\gamma^2\beta^2}{4}(\mathbf{k}_{1,r}+\mathbf{k}_{2,r})^2\right)\\&\quad\times\exp\left(-\frac{\beta^2}{4}(k_{1,z}+k_{1,z})^2\right)\\&\quad\times\int_0^\infty d\tau\exp(-i\beta\Delta\tau-\tau^2),\end{aligned}$$

where $\Delta=\beta(1-\frac{k_1^2+k_2^2}{2})$. This gives

$$M(\mathbf{k}_1,\mathbf{k}_2)=-i\frac{\alpha\beta^2\gamma^2}{16\pi}\exp\left(-\frac{\beta^2}{4}(k_{1,z}+k_{2,z})^2\right)\times\exp\left(-\frac{\gamma^2\beta^2}{4}(\mathbf{k}_{1,r}+\mathbf{k}_{2,r})^2-\frac{\Delta^2}{4}\right)\left[1-\mathrm{erf}\left(\frac{i\Delta}{2}\right)\right]. \tag{8}$$

This expression shows that the anomalous density describes the correlations of atoms with opposite momenta. In other words, it is non-negligible only when $\mathbf{k}_1\simeq-\mathbf{k}_2$. If this condition is not satisfied, the exponential functions drop quickly. Comparing this expression to Eq. (4), we find that the widths of the anomalous density have the same anisotropy and are 2 times larger than the condensate density. Moreover, this expression shows that this function is also non-negligible only for $\Delta\lesssim1$. As β is large, $\Delta\sim1$ only when $k_1\simeq1$ and $k_2\simeq1$. This requirement expresses the conservation of energy in the collision of two atoms.

B. First-order correlation function: $\mathbf{k}_1\simeq\mathbf{k}_2$ correlations

To the lowest order we have

$$G^{(1)}(\mathbf{k}_1,\mathbf{k}_2)=\langle\hat{\delta}^{(1)\dagger}(\mathbf{k}_1)\hat{\delta}^{(1)}(\mathbf{k}_2)\rangle.$$

Using Eq. (7) and $\langle\hat{\delta}^{(0)}(\mathbf{k}_1)\hat{\delta}^{(0)\dagger}(\mathbf{k}_2)\rangle=\delta^{(3)}(\mathbf{k}_1-\mathbf{k}_2)$ we get

$$\begin{aligned}G^{(1)}(\mathbf{k}_1,\mathbf{k}_2)&=|\mathcal{A}|^2\int_0^\infty d\tau\int_0^\infty d\tau'\exp[-\tau^2-\tau'^2+i\beta(\tau-\tau')]\\&\quad\times\int d\mathbf{k}\exp\left[-\frac{\gamma^2\beta^2}{4}[(\mathbf{k}_{1,r}+\mathbf{k}_r)^2+(\mathbf{k}_{2,r}+\mathbf{k}_r)^2]\right]\\&\quad\times\exp\left[-\frac{\beta^2}{4}[(k_{1,z}+k_z)^2+(k_{2,z}+k_z)^2]\right]\\&\quad\times\exp\left[i\frac{\beta}{2}(k^2+k_2^2)\tau'-i\frac{\beta}{2}(k^2+k_1^2)\tau\right].\end{aligned}$$

In Appendix B we show that if the following three conditions are satisfied,

$$\beta \gg 1, \quad \frac{\gamma}{|\mathbf{u}_r|} \ll 1, \quad \frac{1}{|\mathbf{u}_r|\beta\gamma} \ll 1, \tag{9}$$

where $\mathbf{u}=(\mathbf{k}_1+\mathbf{k}_2)/|\mathbf{k}_1+\mathbf{k}_2|$ and $\mathbf{u}_r=(\mathbf{k}_{1,r}+\mathbf{k}_{2,r})/|\mathbf{k}_1+\mathbf{k}_2|$ refers to the radial component of $\mathbf{u}$, then the atomic density is given by

$$G^{(1)}(\mathbf{k},\mathbf{k}) = \frac{\alpha^2\beta\gamma^3}{32\sqrt{2\pi}|\mathbf{u}_r} \exp\left[-\frac{2\beta^2\gamma^2(k-1)^2}{|\mathbf{u}_r|^2}\right] \tag{10}$$

and the first-order correlation function by

$$\begin{aligned} G^{(1)}(\mathbf{k}_1,\mathbf{k}_2) = {} & \frac{\alpha^2\beta\gamma^3}{32\sqrt{2\pi}|\mathbf{u}_r|} \exp\left[-\frac{\gamma^2\beta^2}{8}\Delta\mathbf{k}_r^2 - \frac{\beta^2}{8}\Delta k_z^2\right] \\ & \times \exp\left(-\frac{\beta^2}{8}(\mathbf{u}\Delta\mathbf{k})^2\right)\left[1-\mathrm{erf}\left(\frac{i\beta\mathbf{u}\Delta\mathbf{k}}{2\sqrt{2}}\right)\right] \\ & \times \exp\left(-\frac{2\beta^2\gamma^2\Delta K^2}{\mathbf{u}_r^2}\right). \end{aligned} \tag{11}$$

We have introduced $\frac{|\mathbf{k}_1+\mathbf{k}_2|}{2}=1+\Delta K$, $\Delta\mathbf{k}=\mathbf{k}_1-\mathbf{k}_2$ and assumed $|\Delta\mathbf{k}|$ is small.

The conditions (9) are fulfilled in the experiment of Ref. [3] because the region $u_r \sim 0$ corresponds to the location of the two condensates and has been excluded from the analysis. The density of the scattered particles is peaked around $k=1$ with a width of $\frac{|\mathbf{u}_r|}{\beta\gamma} \ll 1$. We thus expect an anisotropic halo thickness, but the anisotropy is only strong around $u_r \sim 0$, a direction which was inaccessible in the experiment of Ref. [3]

As in the case of the anomalous density M, we can decompose $G^{(1)}(\mathbf{k}_1,\mathbf{k}_2)$ into factors expressing momentum conservation [first line of Eq. (11)] and energy conservation [second line of Eq. (11)]. We find that the widths of the momentum contribution are $\sqrt{2}$ larger than the corresponding ones for $M(\mathbf{k}_1,\mathbf{k}_2)$ [12,18]. As discussed in Refs. [17,18], the $\sqrt{2}$ is due to the assumption of a Gaussian density profile. The energy contribution happens to be much more constraining than for $M(\mathbf{k}_1,\mathbf{k}_2)$ because of the term $\mathbf{u}\Delta\mathbf{k}$. If $\mathbf{u}\Delta\mathbf{k}=0$, meaning $k_1=k_2$, the width of $G^{(1)}(\mathbf{k}_1,\mathbf{k}_2)$ is given by the momentum contribution. But if $\mathbf{u}\Delta\mathbf{k}\neq 0$ and, for instance, if $\mathbf{u}$ is parallel to $\Delta\mathbf{k}$, its width is $\propto 1/\beta$ even in the radial plane, in contradiction with the simple model developed in Ref. [3].

C. Applicability of perturbation theory

Perturbation theory is valid provided the scattering of atoms is spontaneous. When bosonic enhancement comes in to play, the perturbative approach fails. Here we give a simple estimate for parameters such as the number of scattered atoms and the dimensionless parameter β for which the perturbation is small and the above first-order results can be used. Note that, usually, to verify whether the perturbation is small, one has to calculate the physical quantities up to second order. Then, comparison of the two lowest orders would give an answer to the question if the perturbation theory can be used. Moreover, such an approach would yield an expansion parameter in the perturbative series. However, we were unable to evaluate the physical quantities to second order in this case. Thus below we provide an alternative method for verification of whether for these parameters α, β, and γ the perturbative approach applies.

A coherence volume can be attributed to each scattered atom. It is a volume in momentum space in which the atom is first-order coherent. In other words, if we choose a scattered atom with momentum $\mathbf{k}$, the volume set by all the wave vectors $\mathbf{k}_1$ for which $|G^{(1)}(\mathbf{k},\mathbf{k}_1)|$ is not negligible is the coherence volume. If two bosons scatter in such a way that their coherence volumes overlap, their joint detection amplitude is enhanced by an interference effect. In other words, scattering into an already occupied mode is stimulated. The function $G^{(1)}$ permits an estimate of both the number of scattered atoms and their associated coherence volumes. If the number of scattered atoms is small, coherence volumes are unlikely to overlap and stimulated scattering is negligible. In this situation we expect our perturbative solution to be valid.

The above argument was used in the case of the collision of two spherically symmetric ($\gamma=1$) Gaussian wave packets [12] and, in comparisons with numerical solutions of the equation for the field $\hat{\delta}$, proved to be correct. Here we apply an analogous reasoning for the case $\gamma \neq 1$. A conservative estimate for the maximum number of scattered atoms for which the perturbative approach applies is $N_{\mathrm{crit}}=V/V_c$, where V is a lower bound on the k-space volume into which atoms are scattered and V_c is an upper bound on the coherence volume of an individual atom.

In the comparison with the experiment (Sec. IV) we analyze a k-space volume Ω which excludes angles θ smaller than $\pi/4$. From Eq. (10) one sees that the density of scattered atoms is peaked around $k=1$ with an rms width of $\sin\theta/\gamma\beta$. In the volume Ω, the minimum rms width of the shell is $(\gamma\beta\sqrt{2})^{-1}$. Taking twice this minimum rms as the thickness of the shell, we find a lower limit on the volume of $V > 4\pi/\gamma\beta$.

The analysis of Eq. (11) shows that V_c reaches its maximum in Ω for $\theta \simeq \pi/4$ (or $\theta \simeq 3\pi/4$, but due to symmetry we will focus on one of these values). If we set $\theta=\pi/4+\delta\theta$, $\varphi=\delta\varphi$, and $k_1=k_2=1$, we find

$$G^{(1)}(\theta,\varphi) \propto \exp\left(-\frac{\beta^2(\delta\theta)^2}{16} - \frac{\beta^2\gamma^2(\delta\varphi)^2}{16}\right).$$

This gives an angular area of coherence approximately equal to $8\pi/\gamma\beta^2$. Now we need to find the coherence width in the radial direction. Setting $\mathbf{k}_1=(1+\delta k/2)\mathbf{k}/k$ and $\mathbf{k}_2=(1-\delta k/2)\mathbf{k}/k$ we get

$$G^{(1)}(\delta k) \propto \exp\left(-\frac{\beta^2\delta k^2}{8}\right).$$

The limit on the coherence volume is therefore $V_c < 64\pi/3\gamma\beta^3$.

Combining the estimates of V and V_c, we find that the critical number of atoms is given by $N_{\mathrm{crit}}=\frac{3\beta^2}{16}$. For $\beta=227$ we get $N_{\mathrm{crit}} \approx 10^4$. In the experimental realization, the number of atoms detected in Ω varied from 30 to 300. Assuming 10% detection efficiency this gives a maximum of 3000 scat-

tered atoms. Thus the experiment should be in the perturbative regime. A similar argument is given in Ref. [17] leading to a similar value of N_{crit}.

IV. COMPARISON WITH EXPERIMENT

The formulas (8) and (11) cannot be directly compared with experimental data. This is due to an extra step which is made during the measurements: the joint probabilities measured in experiment are averaged over a region of interest Ω which excludes the unscattered condensates. We approximate Ω by $\theta \in [\frac{\pi}{4}, \frac{3\pi}{4}]$ and $\varphi \in [0, 2\pi]$ [where $\mathbf{u} = (\sin\theta\cos\varphi, \sin\theta\sin\varphi, \cos\theta)$].

In case of local momentum correlations, the normalization procedure is done by choosing $\mathbf{k}_1$ and $\mathbf{k}_2$ almost equal: $\mathbf{k}_1 - \mathbf{k}_2 = \delta\mathbf{k}$, where $\delta\mathbf{k}$ is small. So we set $\mathbf{k}_1 = \mathbf{k} + \delta\mathbf{k}/2$ and $\mathbf{k}_2 = \mathbf{k} - \delta\mathbf{k}/2$. The averaging corresponds to calculation of an integral

$$\langle |G^{(1)}(\delta\mathbf{k})|^2 \rangle = \int_\Omega d\mathbf{k} |G^{(1)}(\mathbf{k}_1, \mathbf{k}_2)|^2. \tag{12}$$

Then, this function is normalized by

$$\int_\Omega d\mathbf{k} G^{(1)}(\mathbf{k}_1, \mathbf{k}_1) \cdot G^{(1)}(\mathbf{k}_2, \mathbf{k}_2). \tag{13}$$

Let us denote the resulting normalized function by $\langle |g^{(1)}(\delta\mathbf{k})|^2 \rangle$. As the anomalous density vanishes for local correlations, Eq. (6) gives

$$g^{(2)}(\delta\mathbf{k}) = 1 + \langle |g^{(1)}(\delta\mathbf{k})|^2 \rangle.$$

For $\delta\mathbf{k} = 0$ we get $g^{(2)}(0) = 2$ [18].

In the case of back-to-back momentum correlations, in analogy we have $\mathbf{k}_1$ and $\mathbf{k}_2$ almost opposite: $\mathbf{k}_1 + \mathbf{k}_2 = \delta\mathbf{k}$. We set $\mathbf{k}_1 = \mathbf{k} + \delta\mathbf{k}/2$ and $\mathbf{k}_2 = -\mathbf{k} + \delta\mathbf{k}/2$. Once again, the averaging corresponds to

$$\langle |M(\delta\mathbf{k})|^2 \rangle = \int_\Omega d\mathbf{k} |M(\mathbf{k}_1, \mathbf{k}_2)|^2.$$

After normalization by the function (13) we obtain $\langle |m(\delta\mathbf{k})|^2 \rangle$. For the opposite momentum correlations, $G^{(1)}$ vanishes; thus,

$$g^{(2)}(\delta\mathbf{k}) = 1 + \langle |m(\delta\mathbf{k})|^2 \rangle.$$

Let us now calculate the normalization function from (13), as is common for both local- and opposite-momentum correlations. From Eq. (11) we have

$$G^{(1)}(\mathbf{k}_{1,2}) = \frac{\alpha^2\beta\gamma^3\sqrt{\pi}}{32\pi\sqrt{2}|\mathbf{u}_{1,2r}|} \exp\left[-\frac{\beta^2\gamma^2(k_{1,2}^2 - 1)^2}{2|\mathbf{u}_{1,2r}|^2} \right].$$

Now, in spherical coordinates, $|\mathbf{u}_{1,2r}| = |\sin\theta_{1,2}|$, where $\theta_{1,2}$ is an angle between the vector $\mathbf{k}_{1,2}$ and z axis. Since $\frac{1}{2}\delta\mathbf{k}$ is much smaller than $\mathbf{k}$, we can approximate $\sin\theta_{1,2} \simeq \sin\theta$, where θ is an angle between the vector $\mathbf{k}$ and z axis and drop higher-order terms in $\delta\mathbf{k}$ in the exponentials. We end up with the approximate expression

$$\int_\Omega d\mathbf{k} G^{(1)}(\mathbf{k}_1, \mathbf{k}_1) \cdot G^{(1)}(\mathbf{k}_2, \mathbf{k}_2) \simeq \frac{\alpha^4\beta^2\gamma^6}{2^{11}\pi\sin^2\theta} \int_\Omega d\mathbf{k} \exp\left[-\frac{\beta^2\gamma^2(k^2 - 1)^2}{\sin^2\theta} - \frac{\beta^2\gamma^2(\mathbf{k}\cdot\delta\mathbf{k})^2}{\sin^2\theta} \right].$$

If $\delta\mathbf{k} = \delta k \cdot \mathbf{e}_x$, $\mathbf{k}\cdot\delta\mathbf{k} = k\delta k \sin\theta\cos\phi$, and if $\delta\mathbf{k} = \delta k \cdot \mathbf{e}_z$, $\mathbf{k}\cdot\delta\mathbf{k} = k\delta k\cos\theta$. The resulting integrals are calculated numerically.

A. Back-to-back momentum correlations

As discussed above, we set $\mathbf{k}_1 = \mathbf{k} + \delta\mathbf{k}/2$ and $\mathbf{k}_2 = -\mathbf{k} + \delta\mathbf{k}/2$. Using Eq. (8),

$$|M(\mathbf{k}_1, \mathbf{k}_2)|^2 = \frac{\alpha^2\beta^4\gamma^4}{256\pi^2} \exp\left(-\frac{\gamma^2\beta^2}{2}\delta k_r^2 - \frac{\beta^2}{2}\delta k_z^2 - \frac{\Delta^2}{4} \right) \times \left[1 + \mathrm{erfi}^2\left(\frac{\Delta}{2} \right) \right].$$

Here, $\Delta = \beta(1 - k^2 - \frac{\delta k^2}{4})$. The averaging over Ω is equivalent to

$$\langle |M(\delta\mathbf{k})|^2 \rangle = \int_\Omega d\mathbf{k} |M(\mathbf{k}_1, \mathbf{k}_2)|^2 = \frac{\alpha^2\beta^4\gamma^4}{256\pi^2} e^{-(\gamma^2\beta^2/2)\delta k_r^2} e^{-\beta^2/2\delta k_z^2} \times \int_\Omega d\mathbf{k} e^{-\Delta^2/4} \left[1 + \mathrm{erfi}^2\left(\frac{\Delta}{2} \right) \right].$$

Numerical evaluation of this integral (for parameters β and γ as defined above) shows that the averaged anomalous density can be well approximated by

$$\langle |M(\delta\mathbf{k})|^2 \rangle \propto \exp\left(-\frac{\gamma^2\beta^2}{2}\delta k_r^2 - \frac{\beta^2}{2}\delta k_z^2 \right).$$

As we see, the width of $\langle |M(\delta\mathbf{k})|^2 \rangle$ is primarily determined by the momentum conservation constraint, but the analysis shows that energy conservation plays a role, decreasing the predicted width in the xy plane by the order of 10%. We normalize the second-order correlation function by (13) and introduce an empirical parameter η_{bb} to normalize the height of the calculated correlation function to that of the data. We recall that the experimentally observed heights involve complex issues such as detector resolution, and we refer the reader to Ref. [3] for more information. It is not our purpose to account for the heights here; thus, our empirical parameter is simply a means to compare experimental and theoretical widths.

We find

$$g^{(2)}(\delta\mathbf{k}) = 1 + \eta_{\mathrm{bb}} \langle |m(\delta\mathbf{k})|^2 \rangle.$$

This function is plotted in Fig. 2, using the value $\eta_{\mathrm{bb}} = 0.032$. We find good agreement with the experimental data

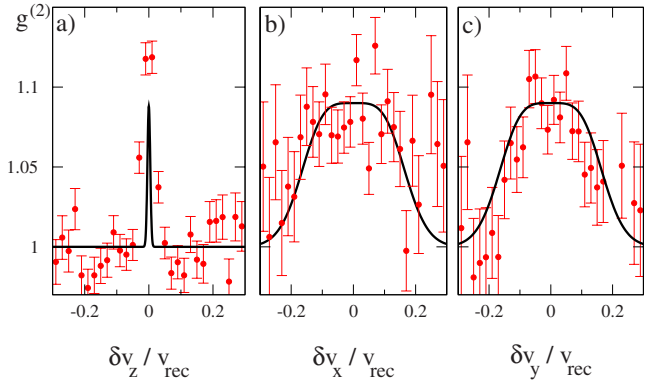

FIG. 2. (Color online) Normalized opposite-momentum correlations calculated in perturbative regime as compared with experimental data. Three plots correspond to three different directions. Here, $\delta v_i=(\hbar/m)\delta k_i$ and $v_{\rm rec}=(\hbar/m)Q$.

in the x and y directions. In the z direction, the width of the experimental peak is dominated by the detector resolution which is larger than the calculated width.

B. Local momentum correlations

For the collinear correlation function we choose $\mathbf{k}_1=\mathbf{k}+\delta\mathbf{k}/2$ and $\mathbf{k}_2=\mathbf{k}-\delta\mathbf{k}/2$. Using Eq. (11) and the definition from Eq. (12) we have

$$\langle|G^{(1)}(\delta\mathbf{k})|^2\rangle=\int_\Omega d\mathbf{k}\frac{\alpha^4\beta^2\gamma^6}{2^{11}\pi|\mathbf{u}_r|^2}\exp\left(-\frac{\beta^2}{4}(\mathbf{u}\delta\mathbf{k})^2\right)\times\exp\left[-\frac{\gamma^2\beta^2}{4}\delta\mathbf{k}_r^2-\frac{\beta^2}{4}\delta k_z^2\right]\times\left[1+\mathrm{erfi}^2\left(\frac{\beta}{2\sqrt{2}}\mathbf{u}\delta\mathbf{k}\right)\right]\times\exp\left(-\frac{4\beta^2\gamma^2(k-1)^2}{\mathbf{u}_r^2}\right).$$

Let us now consider two separate cases.

Let us set $\delta\mathbf{k}=\delta k_x\mathbf{e}_x$. Then, $\mathbf{u}\delta\mathbf{k}=\delta k\sin\theta\cos\varphi$. Integration over the region Ω consists of an angular and a radial integral. The radial one is

$$I_r=\int_0^\infty k^2dk\exp\left(-\frac{4\beta^2\gamma^2(k-1)^2}{\mathbf{u}_r^2}\right).$$

The width of this Gaussian function is so small that we can set $k^2dk\sim dk$. Setting $k=1+dk$ and extending the lower limit of the integral to $-\infty$ gives $I_r\propto|\mathbf{u}_r|$. Thus

$$\langle|G^{(1)}(\delta k_x)|^2\rangle\propto e^{-(\gamma^2\beta^2/4)\delta k_x^2}\int_0^{2\pi}d\varphi\int_{\pi/4}^{3/4\pi}d\theta\times\exp\left(-\frac{\beta^2}{4}\delta k_x^2u^2(\theta,\varphi)\right)\times\left[1+\mathrm{erfi}^2\left(\frac{\beta\delta k_x}{2\sqrt{2}}u(\theta,\varphi)\right)\right],$$

where $u(\theta,\varphi)=\sin\theta\cos\varphi$. This integral is calculated numerically, and we obtain

$$\langle g^{(2)}(\delta k_x)\rangle=1+\langle|g^{(1)}(\delta k_x)|^2\rangle.$$

The result is again rescaled by the parameter η_{cl}, although it need not be identical to the back-to-back case:

$$\langle g^{(2)}(\delta k_x)\rangle=1+\eta_{cl}\langle|g^{(1)}(\delta k_x)|^2\rangle.$$

As $\langle|g^{(1)}(0)|^2\rangle=1$, we deduce the value of $\eta_{\rm cl}=0.05$.

Now we set $\delta\mathbf{k}=\delta k_z\mathbf{e}_z$, and therefore $\mathbf{u}\delta\mathbf{k}=\delta k_z\cos\theta$. The radial integral is the same as in the previous case, and we find

$$\langle|G^{(1)}(\delta k_z)|^2\rangle\propto\exp\left[-\frac{\beta^2}{4}(\delta k_z)^2\right]\times\int_{\pi/4}^{3/4\pi}d\theta\exp\left(-\frac{\beta^2}{4}(\delta k_z)^2\cos^2\theta\right)\times\left[1+\mathrm{erfi}^2\left(\frac{\beta\delta k_z}{2\sqrt{2}}\cos\theta\right)\right].$$

Numerically we find

$$\langle g^{(2)}(\delta k_z)\rangle=1+\eta_{\rm cl}\langle|g^{(1)}(\delta k_z)|^2\rangle.$$

We find that choosing $\eta_{\rm cl}=0.05$ makes the observed heights match.

Once again, because of the detector resolution, we find that the calculated peak is much narrower than the observed one in the z direction. What is more surprising is that the widths of the correlation functions in the x and y directions are also narrower than those in the experiment. As can be seen from the discussion following Eq. (11), the peak width along the direction of the outgoing atoms is strongly constrained by the energy conservation requirement. This means that for scattering far from the z axis (θ large), the x and y components of the correlation function are narrower than they would be taking momentum conservation alone into account. This result contradicts the simple reasoning of Ref. [3].

In the next section we speculate about why the above width for the correlation function is in agreement with neither the experiment nor the positive-P simulations.

V. CONCLUSIONS

The perturbative result we have presented here, while rather complex, has the virtue that the results are analytic and permit identification of the physical processes involved in the pair formation process. In particular, the roles of energy and momentum conservation are clearly identified. Our results for the back-to-back correlation are in good agreement with the experiment. On the other hand, the collinear correlation function, as shown in Fig. 3, is in apparent contradiction with both the experiment and with the calculation of Ref. [17]. The perturbative correlation function given in this work is narrower. This discrepancy clearly needs more attention, both theoretical and experimental, but we wish to make some comments about possible causes. First, as discussed in

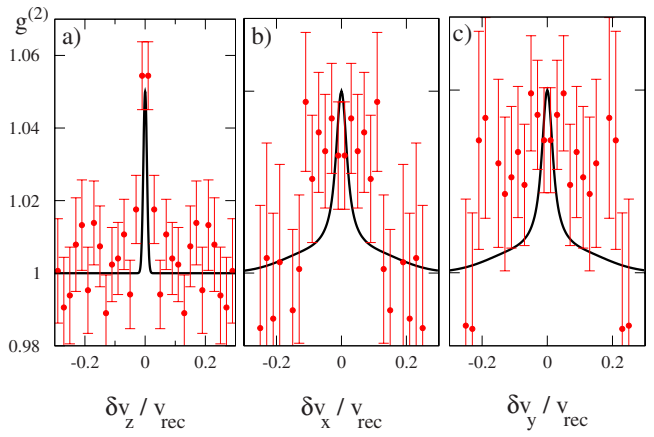

FIG. 3. (Color online) Normalized collinear correlations calculated in the perturbative regime as compared with experimental data. Three plots correspond to three different directions. Due to cylindrical symmetry of the colliding condensates, theoretical results preserve this symmetry. Here, $\delta v_i=(\hbar/m)\delta k_i$ and $v_{\mathrm{rec}}=(\hbar/m)Q$.

Ref. [17], the calculations using the positive-P representation are not able to simulate the entire duration of the collision; indeed, only about 20% of the collision time can be simulated. Thus, energy conservation is not as strictly enforced, leading to additional broadening in the calculations of Ref. [17]. Although this effect was discussed in that reference, the problem requires further scrutiny; it is not entirely clear to us which widths are most affected by a short collision time. Second, the experimental observations are also subject to effects not treated here. It was briefly mentioned in Ref. [3] that the mean-field interaction between the escaping atoms and the remaining condensates may not be negligible. It is therefore important to undertake an analysis of their effect on the correlation functions. Finally, an important simplification in the present treatment is the assumption that the condensates do not expand during the collision. This assumption seems reasonable because most of the atom collisions take place before the clouds have had time to expand. Still, a quantitative estimate of the influence of the condensate expansion is another avenue for future analysis.

Clarifying these questions may have ramifications beyond atom optics. Conceptually similar experiments involving collisions between heavy ions have also uncovered discrepancies between observations and simple models [27,28], the so-called "HBT puzzle." We hope that the work presented here will continue to stimulate careful thought about the four-wave-mixing process of matter waves.

ACKNOWLEDGMENTS

We acknowledge the support of the CIGMA project of the Eurocores program of ESF, the SCALA project of the EU, and the Institut Francilien pour la Recherche en Atomes Froids. P.Z. and J.Ch. acknowledge the support of a Polish Government scientific grant.

APPENDIX A: DETERMINATION OF α

When we introduced α, it was simply defined in terms of the number of atoms, the condensate size, and the scattering length. Here we give a complementary estimate of α which provides a consistency check. The result essentially shows that our treatment is able to predict, to within experimental uncertainties, the number of scattered atoms. We start from Eq. (10). The integration of this equation over Ω gives the number of scattered atoms to first order. This result, being a function of α, can be compared with the number of scattered atoms in the experiment. Knowing this number, we can evaluate α. First, using Eq. (10), the number of scattered atoms in Ω is given by

$$\mathcal{N}_\Omega=\frac{\alpha^2\beta\gamma^3}{32\sqrt{2\pi}|\mathbf{u}_r|}\int_\Omega d\mathbf{k}\,\exp\left[-\frac{\beta^2\gamma^2(k^2-1)^2}{2|\mathbf{u}_r|^2}\right].$$

Let us focus for a moment on the radial part of the above integral:

$$I_{\mathrm{rad}}=\frac{\alpha^2\beta\gamma^3}{32\sqrt{2\pi}|\mathbf{u}_r|}\int_0^\infty k^2dk\,\exp\left[-\frac{\beta^2\gamma^2(k^2-1)^2}{2|\mathbf{u}_r|^2}\right].$$

First, as the integrand is strongly peaked around $k=1$, the measured volume can be dropped; i.e., $k^2\sim 1$. Then, introducing $k=1+\delta k$ and assuming δk is small we get

$$I_{\mathrm{rad}}\simeq\frac{\alpha^2\beta\gamma^3}{32\sqrt{2\pi}|\mathbf{u}_r|}\int_{-1}^\infty d(\delta k)\exp\left[-\frac{2\beta^2\gamma^2(\delta k)^2}{|\mathbf{u}_r|^2}\right].$$

The lower limit can be extended to $-\infty$, giving

$$I_{\mathrm{rad}}\simeq\frac{\alpha^2\beta\gamma^3}{32\sqrt{2\pi}|\mathbf{u}_r|}\int_{-\infty}^\infty d(\delta k)\exp\left[-\frac{2\beta^2\gamma^2(\delta k)^2}{|\mathbf{u}_r|^2}\right]=\frac{\alpha^2\gamma^2}{64}.$$

Integration over the angular variables gives a factor of $2\sqrt{2}\pi$ and

$$\mathcal{N}_\Omega=\frac{\pi\sqrt{2}}{32}\alpha^2\gamma^2.$$

From the experimental data we know that the number of scattered atoms varies from 300 to 3000. For $N_\Omega=300$ we get $\alpha=930$, and for $N_\Omega=3000$ we get $\alpha=2940$. Thus the value of $\alpha=1652$ calculated from the model of colliding Gaussians lies somewhere in between. This result confirms that the choice of parameters such as σ_r and σ_z is reasonable.

APPENDIX B: FIRST-ORDER CORRELATION FUNCTION: $\mathbf{k}_1\simeq\mathbf{k}_2$ CORRELATIONS

To first order the $G^{(1)}$ function is

$$G^{(1)}(\mathbf{k}_1,\mathbf{k}_2)=|\mathcal{A}|^2\int_0^\infty d\tau\int_0^\infty d\tau'\,\exp[-\tau^2-\tau'^2+i\beta(\tau-\tau')]$$
$$\times\int d\mathbf{k}\,\exp\left[-\frac{\gamma^2\beta^2}{4}[(\mathbf{k}_{1,r}+\mathbf{k}_r)^2+(\mathbf{k}_{2,r}+\mathbf{k}_r)^2]\right]$$

$$\times\exp\left[-\frac{\beta^2}{4}[(k_{1,z}+k_z)^2+(k_{2,z}+k_z)^2]\right]$$
$$\times\exp\left[i\frac{\beta}{2}(k^2+k_2^2)\tau'-i\frac{\beta}{2}(k^2+k_1^2)\tau\right].$$

Thus, in contrast to the anomalous density, we must perform a two fold time as well as a three-dimensional space integral. The space integral can be evaluated analytically. Then, introducing $x=\frac{\tau+\tau'}{\sqrt{2}}$ and $y=\frac{\tau-\tau'}{\sqrt{2}}$ the first-order correlation function is

$$G^{(1)}(\mathbf{k}_1,\mathbf{k}_2)=\frac{\alpha^2\beta\gamma^2}{16\pi^{3/2}\sqrt{2}}\exp\left[-\frac{\gamma^2\beta^2}{8}|\mathbf{k}_{1,r}-\mathbf{k}_{2,r}|^2-\frac{\beta^2}{8}|k_{1,z}-k_{2,z}|^2\right]\int_0^\infty dx\int_{-x}^{x}dy\exp\left[-x^2+i\frac{\beta}{2\sqrt{2}}x(k_2^2-k_1^2)\right]$$
$$\times\exp\left[-y^2\left(1+\frac{\mathbf{u}_r^2}{\gamma^2}+\mathbf{u}_z^2\right)+i\beta\sqrt{2}y\left(1-\frac{k_1^2+k_2^2}{4}-\frac{(\mathbf{k}_1+\mathbf{k}_2)^2}{8}\right)\right]\exp\left[i\sqrt{2}y\frac{(\mathbf{k}_{1,r}+\mathbf{k}_{2,r})^2}{4}\frac{y^2}{\gamma^2(\beta\gamma^2)}\frac{1}{1+2y^2/(\beta\gamma^2)^2}\right]$$
$$\times\exp\left[\frac{y^2}{\gamma^2}\left(\mathbf{u}_r^2-\frac{(\mathbf{k}_{1,r}+\mathbf{k}_{2,r})^2}{4[1+2y^2/(\beta\gamma^2)^2]}\right)\right]\exp\left[i\sqrt{2}y\frac{(k_{1,z}+k_{2,z})^2}{4}\frac{y^2}{\beta}\frac{1}{1+2y^2/\beta^2}\right]$$
$$\times\exp\left[y^2\left(\mathbf{u}_z^2-\frac{(\mathbf{k}_{1,r}+\mathbf{k}_{2,r})^2}{4(1+2y^2/\beta^2)}\right)\right]\frac{1}{1+i\sqrt{2}y/(\beta\gamma^2)}\frac{1}{\sqrt{1+i\sqrt{2}y/\beta}},$$

where $\mathbf{u}=\mathbf{u}_r+\mathbf{u}_z$ is a vector of unit length and direction $\mathbf{k}_1+\mathbf{k}_2$. As the scattering of atoms conserves energy and momentum, we expect that the density of atoms should be centered around $|\mathbf{k}|=1$ (which corresponds to $|\mathbf{k}|=Q$ in physical units). Moreover, from the factor $\exp[-y^2(1+\frac{\mathbf{u}_r^2}{\gamma^2}+\mathbf{u}_z^2)]$, we deduce that the characteristic width of variable y is $1/\sqrt{1+\frac{\mathbf{u}_r^2}{\gamma^2}+\mathbf{u}_z^2}$.

Using the second of conditions (9) we have

$$\exp\left[-y^2\left(1+\frac{\mathbf{u}_r^2}{\gamma^2}+\mathbf{u}_z^2\right)\right]\simeq\exp\left[-y^2\frac{\mathbf{u}_r^2}{\gamma^2}\right].$$

Since the characteristic range of y is $\gamma/|\mathbf{u}_r|$, all the terms proportional to y/β and $y/\beta\gamma^2$ can be dropped. This gives

$$G^{(1)}(\mathbf{k}_1,\mathbf{k}_2)=\frac{\alpha^2\beta\gamma^2}{16\pi^{3/2}\sqrt{2}}$$
$$\times\exp\left[-\frac{\gamma^2\beta^2}{8}|\mathbf{k}_{1,r}-\mathbf{k}_{2,r}|^2-\frac{\beta^2}{8}|k_{1,z}-k_{2,z}|^2\right]$$
$$\times\int_0^\infty dx\int_{-x}^{x}dy\exp\left[-x^2+i\frac{\beta}{2\sqrt{2}}x(k_2^2-k_1^2)\right]$$
$$\times\exp\left[-\frac{y^2}{\gamma^2}\mathbf{u}_r^2+i\beta\sqrt{2}y\left(1-\frac{k_1^2+k_2^2}{4}-\frac{(\mathbf{k}_1+\mathbf{k}_2)^2}{8}\right)+\frac{y^2}{\gamma^2}\left(\mathbf{u}_r^2-\frac{(\mathbf{k}_{1,r}+\mathbf{k}_{2,r})^2}{4}\right)\right].\tag{B1}$$

Now, by letting $\mathbf{k}_1=\mathbf{k}_2=\mathbf{k}$ in Eq. (B1) let us focus on the momentum density of scattered atoms:

$$G^{(1)}(\mathbf{k},\mathbf{k})=\frac{\alpha^2\beta\gamma^2}{16\pi^{3/2}\sqrt{2}}\int_0^\infty dx\exp[-x^2]\int_{-x}^{x}dy\exp\left[-\frac{y^2}{\gamma^2}\mathbf{u}_r^2+i\beta\sqrt{2}y(1-k^2)\right]\exp\left[\frac{y^2}{\gamma^2}\mathbf{u}_r^2(1-k^2)\right].$$

From the above we deduce that the characteristic width of x is 1, which is much larger that the characteristic width of y. This allows another approximation—the limits of y integral can be expanded up from $-\infty$ to ∞. The variables y and x effectively decouple, giving

$$G^{(1)}(\mathbf{k},\mathbf{k})=\frac{\alpha^2\beta\gamma^2}{32\pi\sqrt{2}}\int_{-\infty}^{\infty}\exp\left[-\frac{y^2}{\gamma^2}\mathbf{u}_r^2+i\beta\sqrt{2}y(1-k^2)\right]\times\exp\left[\frac{y^2}{\gamma^2}\mathbf{u}_r^2(1-k^2)\right]dy.$$

After integration over y and with $k\sim 1$, one obtains

$$G^{(1)}(\mathbf{k},\mathbf{k})=\frac{\alpha^2\beta\gamma^3}{32\sqrt{2\pi}|\mathbf{u}_r|}\exp\left[-\frac{2\beta^2\gamma^2(k-1)^2}{|\mathbf{u}_r|^2}\right].$$

Equation (B1) can be rewritten in the form

$$G^{(1)}(\mathbf{k}_1,\mathbf{k}_2)=\frac{\alpha^2\beta\gamma^2}{16\pi^{3/2}\sqrt{2}}$$
$$\times\exp\left[-\frac{\gamma^2\beta^2}{8}|\mathbf{k}_{1,r}-\mathbf{k}_{2,r}|^2-\frac{\beta^2}{8}|k_{1,z}-k_{2,z}|^2\right]$$
$$\times\int_0^\infty dx\int_{-x}^{x}dy\exp\left[-x^2+i\frac{\beta}{2\sqrt{2}}x(k_2^2-k_1^2)\right]$$
$$\times\exp\left[-\frac{y^2}{\gamma^2}\mathbf{u}_r^2+i\beta\sqrt{2}y\left(1-\frac{k_1^2+k_2^2}{4}\right.\right.$$

$$-\frac{(\mathbf{k}_1+\mathbf{k}_2)^2}{8}\Bigg)+\frac{y^2}{\gamma^2}\Bigg(\mathbf{u}_r^2-\frac{(\mathbf{k}_{1,r}+\mathbf{k}_{2,r})^2}{4}\Bigg)\Bigg].$$

Introducing $\frac{|\mathbf{k}_1+\mathbf{k}_2|}{2}=1+\Delta K$ and $\Delta\mathbf{k}=\mathbf{k}_1-\mathbf{k}_2$, where $|\Delta\mathbf{k}|$ is small, we obtain

$$G^{(1)}(\mathbf{k}_1,\mathbf{k}_2)=\frac{\alpha^2\beta\gamma^3}{32\sqrt{2\pi}|\mathbf{u}_r|}\exp\Bigg[-\frac{\gamma^2\beta^2}{8}\Delta\mathbf{k}_r^2-\frac{\beta^2}{8}\Delta k_z^2\Bigg]\times\exp\Bigg(-\frac{\beta^2}{8}(\mathbf{u}\Delta\mathbf{k})^2-\frac{2\beta^2\gamma^2\Delta K^2}{\mathbf{u}_r^2}\Bigg)\times\Bigg[1-\mathrm{erf}\Bigg(\frac{i\beta\mathbf{u}\Delta\mathbf{k}}{2\sqrt{2}}\Bigg)\Bigg].$$

[1] D. C. Burnham and D. L. Weinberg, Phys. Rev. Lett. **25**, 84 (1970).
[2] M. Greiner, C. A. Regal, J. T. Stewart, and D. S. Jin, Phys. Rev. Lett. **94**, 110401 (2005).
[3] A. Perrin, H. Chang, V. Krachmalnicoff, M. Schellekens, D. Boiron, A. Aspect, and C. I. Westbrook, Phys. Rev. Lett. **99**, 150405 (2007).
[4] L.-M. Duan, A. Sørensen, J. I. Cirac, and P. Zoller, Phys. Rev. Lett. **85**, 3991 (2000).
[5] H. Pu and P. Meystre, Phys. Rev. Lett. **85**, 3987 (2000).
[6] T. Opatrný and G. Kurizki, Phys. Rev. Lett. **86**, 3180 (2001).
[7] K. V. Kheruntsyan, M. K. Olsen, and P. D. Drummond, Phys. Rev. Lett. **95**, 150405 (2005).
[8] A. Vardi and M. G. Moore, Phys. Rev. Lett. **89**, 090403 (2002).
[9] R. Bach, M. Trippenbach, and K. Rzążewski, Phys. Rev. A **65**, 063605 (2002).
[10] V. A. Yurovsky, Phys. Rev. A **65**, 033605 (2002).
[11] P. Ziń, J. Chwedeńczuk, A. Veitia, K. Rzążewski, and M. Trippenbach, Phys. Rev. Lett. **94**, 200401 (2005).
[12] P. Ziń, J. Chwedeńczuk, and M. Trippenbach, Phys. Rev. A **73**, 033602 (2006).
[13] A. A. Norrie, R. J. Ballagh, and C. W. Gardiner, Phys. Rev. Lett. **94**, 040401 (2005).
[14] A. A. Norrie, R. J. Ballagh, and C. W. Gardiner, Phys. Rev. A **73**, 043617 (2006).
[15] C. M. Savage, P. E. Schwenn, and K. V. Kheruntsyan, Phys. Rev. A **74**, 033620 (2006).
[16] P. Deuar and P. D. Drummond, Phys. Rev. Lett. **98**, 120402 (2007).
[17] A. Perrin, C. M. Savage, D. Boiron, V. Krachmalnicoff, C. I. Westbrook, and K. V. Kheruntsyan, New J. Phys. **10**, 045021 (2008).
[18] K. Mølmer, A. Perrin, V. Krachmalnicoff, V. Leung, D. Boiron, A. Aspect, and C. I. Westbrook, Phys. Rev. A **77**, 033601 (2008).
[19] A. P. Chikkatur, A. Görlitz, D. M. Stamper-Kurn, S. Inouye, S. Gupta, and W. Ketterle, Phys. Rev. Lett. **85**, 483 (2000).
[20] K. Gibble, S. Chang, and R. Legere, Phys. Rev. Lett. **75**, 2666 (1995).
[21] N. Katz, E. Rowen, R. Ozeri, and N. Davidson, Phys. Rev. Lett. **95**, 220403 (2005).
[22] M. Schellekens, R. Hoppeler, A. Perrin, J. Viana Gomes, D. Boiron, C. I. Westbrook, and A. Aspect, Science **310**, 648 (2005).
[23] T. Jeltes, J. M. McNamara, W. Hogervorst, W. Vassen, V. Krachmalnicoff, M. Schellekens, A. Perrin, H. Chang, D. Boiron, A. Aspect *et al.*, Nature (London) **445**, 402 (2007).
[24] M. O. Scully and M. S. Zubairy, *Quantum Optics*, 1st ed. (Cambridge University Press, Cambridge, England, 1997).
[25] E. M. Lifshitz and L. P. Pitaevskii, *Statistical Physics* (Pergamon Press, Oxford, 1980), Pt. 2.
[26] P. Öhberg, E. L. Surkov, I. Tittonen, S. Stenholm, M. Wilkens, and G. V. Shlyapnikov, Phys. Rev. A **56**, R3346 (1997).
[27] M. Lisa, S. Pratt, R. Stoltz, and U. Wiedemann, Annu. Rev. Nucl. Part. Sci. **55**, 357 (2005).
[28] C.-Y. Wong and W.-N. Zhang, Phys. Rev. C **76**, 034905 (2007).